

C-H. Su¹, H-S. Sheu², Y-W. Lo³, J-C. Weng¹, D-B. Shieh⁴, C-S. Yeh³, and J-H. Chen¹

¹Interdisciplinary MRI/MRS Lab, Department of Electrical Engineering, National Taiwan University, Taipei, Taiwan, ²National Synchrotron Radiation Research Center, Hsinchu, Taiwan, ³Department of Chemistry, National Cheng Kung University, Tainan, Taiwan, ⁴Institute of Oral Medicine and Molecular Medicine, National Cheng Kung University, Tainan, Taiwan

Introduction

Nanoparticle systems are promising new paradigms in pharmacotherapy and provide many applications in the areas of gene therapy, drug delivery [1], imaging [2], and novel drug discovery techniques [3]. The aim of nanodiagnosics is to identify disease at its earliest stage, particularly at the molecular level. Nanoparticle-based molecular imaging has set a unique platform for cellular tracking, targeted diagnostic studies, and image-monitored therapy. Magnetic resonance imaging (MRI) has been recognized as the most important development in medical diagnosis since the discovery of the X-ray. MRI measures the characteristics of the hydrogen nuclei of water and gives spatial distribution of the intensity of water protons. The signal intensity depends on the amount of water in the image area. Contrast agents accelerate the rate of relaxation of nearby water molecules, thereby greatly increasing the contrast between the specific tissue or organ of interest and surrounding tissue. The effective MR contrast agents must have a strong effect to accelerate spin-lattice relaxation (T₁), which produces bright or positive contrast images, or shorten spin-spin relaxation (T₂), which creates a dark or negative contrast effect. Currently, MR contrast agents can be categorized into T₁-positive agents of paramagnetic species and T₂-negative agents of superparamagnetic particles. Recently, some Gd-based nanoparticle contrast agents have also been reported [4]. The superparamagnetic particles (T₂-negative agents) are nano- or sub-micrometer sizes and can be classified as superparamagnetic iron oxide (SPIO), ultrasmall SPIO (USPIO), or monocrystalline iron oxide nanoparticles (MION) [5]. Superparamagnetic particles consist of many magnetic ions with significant, large, unpaired spins; they are superparamagnetic when the magnetic ions are mutually aligned. In this work, we present a new class of bimetallic MR contrast agent: Au₃Cu₁ hollow nanospheres (Scheme 1).

Materials and Methods

Preparing Au₃Cu₁ nanoshells and polyelectrolyte-coated Au₃Cu₁ nanocapsules Cu colloidal solution was added to HAuCl₄ (dehydrated) and was sonicated for 10 min to form Au₃Cu₁ hollow nanospheres. The colloidal color changed almost immediately (< 1 min) from wine-red to grayish blue after it had been added to the HAuCl₄. We added 5 mL of 2-propanol to dilute Au₃Cu₁ colloidal solution before coating polymers with the biocompatible polyelectrolytes polyethylenimine (PEI) and polyacrylic acid (PAA). We have used a layer-by-layer (LbL) method to prepare the PEI/PAA/PEI-coated Au₃Cu₁ nanocapsules.

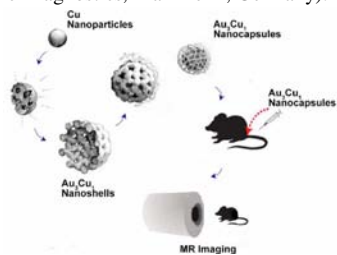
Evaluating the biocompatibility of Au₃Cu₁ nanocapsules and nanoshells coated with PEI/PAA/PEI polymers We used a WST-1 assay on a Vero cell line to measure mitochondrial dehydrogenase activity known to be associated with cell viability and two approaches were performed to evaluate the cytotoxicity of the newly synthesized Au₃Cu₁ nanocapsules and nanoshells *in vitro*. The quantification determining cell viability was done using optical absorbance (450/690 nm) and an ELISA plate reader.

In vitro MR imaging The experiments were done using a spectroscope (3T MRI Biospec; Bruker, Ettlingen, Germany). A gradient system mounted on the table of the 3T magnet with an inner diameter of 6 cm and a maximal gradient strength of 1000 mT m⁻¹ was used to yield high-resolution images. A quadrature coil with an inner diameter of 3.5 cm was used for RF transmission and reception. For *in vitro* MR images and both T₁ and T₂ measurements, all nanoshells and nanocapsules were dispersed in 5% agarose gel of various concentrations. Acquired images had a matrix size of 256 × 192, a field of view of 60 × 60 mm, and a slice thickness of 6 mm yielding an in-plane resolution of 234 μm after image smoothing. T₁ value measurements were done using a multi-slice multi-echo sequence with a repetition time (TR) of 6000 ms, an echo time (TE) of 8.7 ms, and 45 inversion recovery points (TI from 13.3 ms to 6000 ms). The field of view was 60 × 60 mm, the slice thickness was 6 mm, and the image matrix was 128 × 128. This allowed for simultaneous imaging of 26 vials with 0.3 mL of contrast agent for each vial. An average signal of 50 voxels was evaluated for all TI values. T₂ value measurements were performed with a spin echo sequence of TR/TE of 4000/10.1 ms, 60 echo points of 60, and a NEX of 5. The field of view was 60 × 60 mm, the slice thickness was 6 mm, and the imaging plane was 256 × 192.

Results

Biocompatible polyelectrolyte materials, polyethylenimine (PEI) and polyacrylic acid (PAA), are used on the particle surfaces forming polyelectrolyte multilayer nanocapsules. We used a layer-by-layer (LbL) method based on electrostatic attraction between oppositely charged polymer layers to first assemble a positively charged PEI and then a negatively charged PAA layer on Au₃Cu₁ nanoshells (shown in Fig. 1): 3-layer polyelectrolytes (PEI/PAA/PEI), with PEI as the outermost layer in the polyelectrolyte shells, were deposited, and the thickness of the polymer shell was 6.1 ± 1.2 nm.

We then evaluated *in vitro* spin-lattice relaxation time (T₁) weighted images and spin-spin relaxation time (T₂) weighted images in 0.5 % agarose gel for Au₃Cu₁ nanocapsules (Au₃Cu₁ coated with PEI/PAA/PEI) and Au₃Cu₁ nanoshells (not coated with polymers) with different concentrations: 0 (0.5 % agarose gel only), 0.125, 0.25, 1.25, 2.50, and 5.00 mg mL⁻¹ (Fig. 2 and 3). Cell viability experiments were conducted on a vero cell line (monkey kidney cell line) using a WST-1 assay (Roche Diagnostics, Mannheim, Germany). Both Au₃Cu₁ nanocapsules and Au₃Cu₁ nanoshells were delivered over a range (0 ~ 200 μg mL⁻¹) of dosages (Fig. 4).



Scheme 1. The as-prepared Au₃Cu₁ nanocapsules used as the contrast agents in animal MR imaging.

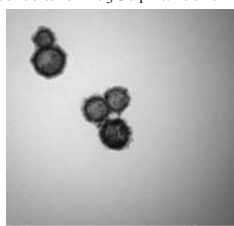


Figure 1 The TEM image of Au₃Cu₁ nanocapsules showing polyelectrolyte shells.

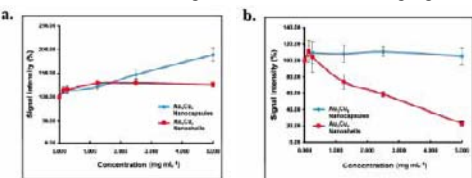


Figure 3 *In vitro* magnetic resonance imaging intensity plots of (a) T₁- and (b) T₂-weighted signals in H₂O/0.5 % agarose gel containing increasing concentrations of Au₃Cu₁ nanocapsules (blue) and nanoshells (red).

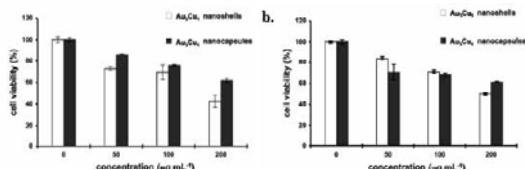


Figure 4 The biocompatibility of the Au₃Cu₁ nanoshells and Au₃Cu₁ nanocapsules. The biocompatibility was analyzed using a WST-1 assay. The nanoshells (white column) or nanocapsules (black column) were coated on the microplate with various dosages (50, 100, 200 μg mL⁻¹) first, followed by adding cells for (a) 6 h and (b) 24 h.

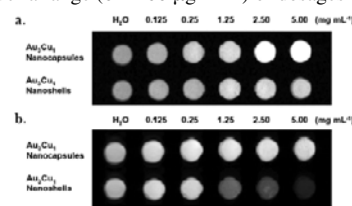


Figure 2 MR *in vitro* assays of Au₃Cu₁ nanocapsules and nanoshells. (a) Multi-slice multi-echo T₁-weighted images of Au₃Cu₁ nanocapsules and nanoshells in water containing 0.5 % agarose gel. (b) Fast spin echo T₂-weighted images of Au₃Cu₁ nanocapsules and nanoshells in water containing 0.5% agarose gel at 125.3 MHz (3T MR system).

Conclusion

The anomalously high oxidation rate of copper, Au₃Cu₁ hollow nanostructures are believed to be the first bimetallic MR contrast agents. Au₃Cu₁ nanocapsules enhanced signal contrast not only in T₁-weighted imaging, but also in T₂-weighted imaging at lower doses, and the increase the brightness of T₂-weighted MR images has resulted in the potential development of this agent for MR angiography. We believed that the cooperativity originating from the form of the nanoparticles and the large surface area of the water because of its porous hollow morphology are primarily involved. Furthermore, the amine groups on the outermost PEI polymer shell of the nanocapsules, which further provides surface modification for the attachment of biological signals, suggest great potential for use in multifunctional composite capsules as functional carriers and imaging agents. Overall, these results might lead to the creation of other non-Gd- and iron oxide-base bimetallic contrast agents.

References

[1] a) Shaffer, C. *Drug Discov. Today* **2005**, *10*, 1581. b) Vinogradov, S. *Expert. Opin. Drug Deliv.* **2004**, *1*, 181. [2] Li, K. C. *et al. Biomed. Microdevices* **2004**, *6*, 113. [3] a) Wilkinson, J. M. *Med. Device Technol.* **2003**, *14*, 29. b) Roco, M. C. *Curr. Opin. Biotechnol.* **2003**, *14*, 337. [4] a) Evancic, F. *et al. Chem. Mater.* **2006**, *18*, 2499. b) Rieter, W. J. *et al. J. Am. Chem. Soc.* **2006**, *128*, 9024. [5] a) Harisinghani, M. G. *et al. N. Engl. J. Med.* **2003**, *348*, 2491. b) Shieh, D. B. *et al. Biomaterials* **2005**, *26*, 7183.